

Separating methane production and consumption with a field-based isotope pool dilution technique

Joseph C. von Fischer¹ and Lars O. Hedin²

Department of Ecology and Evolutionary Biology, Cornell University, Ithaca, New York, USA

Received 7 June 2001; revised 26 February 2002; accepted 26 February 2002; published 12 July 2002.

[1] Despite the importance of methane for climate, it has remained difficult to measure gross rates of methane production and consumption without inducing artifacts. To remedy this, we have developed, tested, and applied a field-based $^{13}\text{CH}_4$ pool dilution technique. Laboratory tests, sensitivity analyses, and field data indicate that this technique is robust for measuring gross rates of methane production and consumption. In our analyses of 130 soil cores from 17 field sites of differing environmental conditions, we encountered a wide range of gross methane production rates ($0.04\text{--}930\text{ mg CH}_4\text{-C m}^{-2}\text{ day}^{-1}$), but encountered a narrower range of consumption rates ($0.1\text{--}9.2\text{ mg CH}_4\text{-C m}^{-2}\text{ day}^{-1}$). Unexpectedly, we found that gross production of methane was common (mean = $0.15\text{ mg CH}_4\text{-C m}^{-2}\text{ day}^{-1}$) even in dry, oxic soils where average soil conditions cannot support methane producers. Through improved measurement of methane turnover in soils, this technique can offer a more fine-grained understanding of how productive and consumptive processes are linked to soil-atmosphere trace gas balances. *INDEX TERMS:* 0315 Atmospheric Composition and Structure: Biosphere/atmosphere interactions; 1615 Global Change: Biogeochemical processes (4805); 1694 Global Change: Instruments and techniques; 4840 Oceanography: Biological and Chemical: Microbiology; *KEYWORDS:* methanogenesis, methanotrophy, isotope pool dilution, anaerobic microsite, soil biogeochemistry, trace gas flux

1. Introduction

[2] Methane is a powerful heat-trapping gas that affects the Earth's climate system [Wang *et al.*, 1976; Cicerone and Oremland, 1988; Harries *et al.*, 2001]. Over the past 400,000 years, atmospheric methane concentrations have generally risen in response to periods of warming, thus amplifying climate change [Petit *et al.*, 1999] and raising questions about potential feedback mechanisms between the biosphere and climate. Over the past 150 years, humans have doubled the concentration of atmospheric methane [Etheridge *et al.*, 1992], primarily through effects on the production of methane within soils and sediments [Cicerone and Oremland, 1988; Lelieveld *et al.*, 1998]. This modern rise is expected to contribute increasingly to anthropogenic climate change [Houghton *et al.*, 1996; Hansen *et al.*, 1998], further underscoring the need to understand the processes that regulate atmospheric methane concentration.

[3] A fundamental and remaining challenge lies in understanding the controls of gross methane production and consumption in soils [e.g., Cicerone and Oremland, 1988; Matthews, 2000; Matthews and Fung, 1987; Potter *et al.*,

1996; Potter, 1997; Walter and Heimann, 2000]. The balance between gross rates of production and consumption determines whether a soil is a net source or sink for atmospheric methane. Waterlogged soils are environments where production often exceeds consumption, accounting for 38% of modern net methane sources and accounting for 68% of preindustrial sources [Lelieveld *et al.*, 1998]. In contrast, well-drained soils generally display net consumption of methane and create a small sink globally for atmospheric methane [Lelieveld *et al.*, 1998]. Changes in soil water content due to climate variations may therefore cause dramatic (and potentially nonlinear) changes in methane emissions to the atmosphere [Matthews, 2000]. These changes, in turn, create feedbacks that depend on how soil methane transformations respond to changes in soil moisture.

[4] It is important to understand gross methane production and consumption separately, because the microbial populations responsible for the two processes are ecologically and evolutionarily very different, and they respond quite differently to environmental controls [Zinder, 1993; Hanson and Hanson, 1996; King, 1997]. Methane production and consumption are typically measured separately by inhibiting one process with chemical inhibitors or by manipulating the soil oxygen status and thus the balance between productive and consumptive processes [e.g., Oremland and Culbertson, 1992a, 1992b; Davidson and Schimel, 1995; Yavitt *et al.*, 1995; King, 1996; Saarnio *et al.*, 1997; Moosavi and Crill, 1998]. However, such inhibition approaches provide only limited understanding of these

¹Now at Department of Geosciences, Princeton University, Princeton, New Jersey, USA.

²Now at Department of Ecology and Evolutionary Biology and Princeton Environmental Institute, Princeton University, Princeton, New Jersey, USA.

processes, because chemical inhibitors can simultaneously affect both processes [Frenzel, 1996; King, 1996] and because the manipulation of oxygen status relies on physical or chemical disruption of the soil-microbe system [Madsen, 1998; Sundh *et al.*, 1994].

[5] To date, techniques that do not involve inhibition have relied on the addition of radiocarbon [e.g., Yavitt *et al.*, 1990; Whalen *et al.*, 1992; Andersen *et al.*, 1998] or interpretation of patterns in the natural abundance of stable isotopes [e.g., Chanton *et al.*, 1997; Liptay *et al.*, 1998; Sugimoto *et al.*, 1998]. Unfortunately, radiocarbon techniques can only be used in the laboratory (but see Wieder and Yavitt [1994] for a rare exception) and are thus subject to time delays between field sampling and analysis and to disturbance to the soils during transport [Madsen, 1998; Sundh *et al.*, 1994]. Natural abundance stable isotope approaches are indirect and highly sensitive to assumptions of methane transport, isotopic fractionation effects, and isotopic signatures of source methane [Snover and Quay, 2000].

[6] Although these techniques have contributed to the general understanding of methane production and consumption, more specific understanding of the soil-microbe system will depend on techniques that can more clearly separate productive and consumptive processes in the field. To this end, we have developed a new technique that permits simultaneous observations of methane production and consumption in the field, based on the approach of stable isotope pool dilution. In this paper, we develop a mathematical model for determining rates of microbial activity from measured mass and isotope data. We use computer simulations and field trials on different soil types to examine the sensitivity of the technique to error in assumptions and analysis. Finally, we examine results from field application of the technique and discuss implications of our method for improved understanding of controls on methane flux and soil microbial ecology.

2. Principles and Mathematical Model

[7] Our technique is based on the principles of isotope pool dilution [Kirkham and Bartholomew, 1954, 1955], which we have adapted to study gross methane production and consumption in soils using trace-level additions of isotopically labeled methane. Here we develop an idealized model assuming a closed system of soil particles and atmosphere where all methane exists in the atmospheric pool, as depicted in Figure 1. The approach depends on measuring changes in the amount of atmospheric methane and the ratio of labeled to unlabeled methane over the course of the soil incubation. From these measured data we can calculate gross methane consumption from the loss of labeled methane over time because, after an initial diffusive redistribution of the added label [Andersen *et al.*, 1998], only consumption affects this amount. Because production generates only unlabeled methane, we can further calculate gross methane production from the dilution of labeled methane over time (i.e., isotope dilution). In the following sections, we (1) describe the equations for changes in the amount of unlabeled methane over time (2) describe the equation for changes in the amount of labeled methane over time, and (3) describe the equation for change

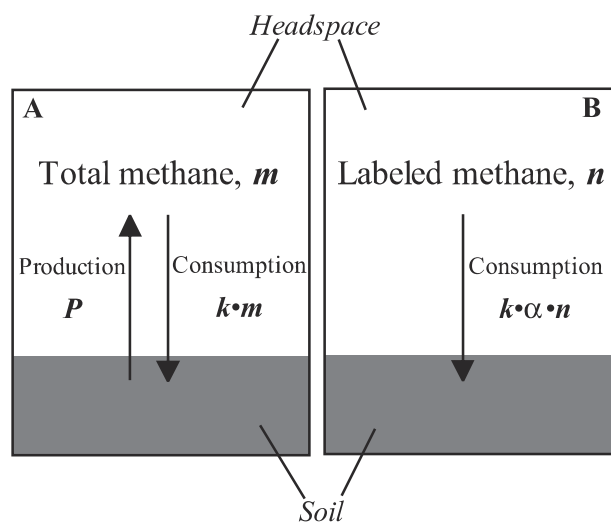


Figure 1. Conceptual diagram of pool dilution approach for measuring gross methane production and consumption using additions of labeled methane molecules (i.e., $^{13}\text{CH}_4$) in a closed system. (a) Simultaneous processes of methane production and consumption that affect total amount of methane. We describe the methane production rate, P , as constant and describe the methane consumption rate as the product of a first-order rate constant, k , and the amount of methane, m . (b) Illustration showing that only methane consumption affects the amount of label, n . Isotopic fractionation slows consumption of label by a constant amount, α . See section 2 for a more detailed treatment of these relationships.

in the ratio of labeled to unlabeled methane over time. We later examine the sensitivity of this idealized model to various assumptions and to potential errors associated with field-based measures.

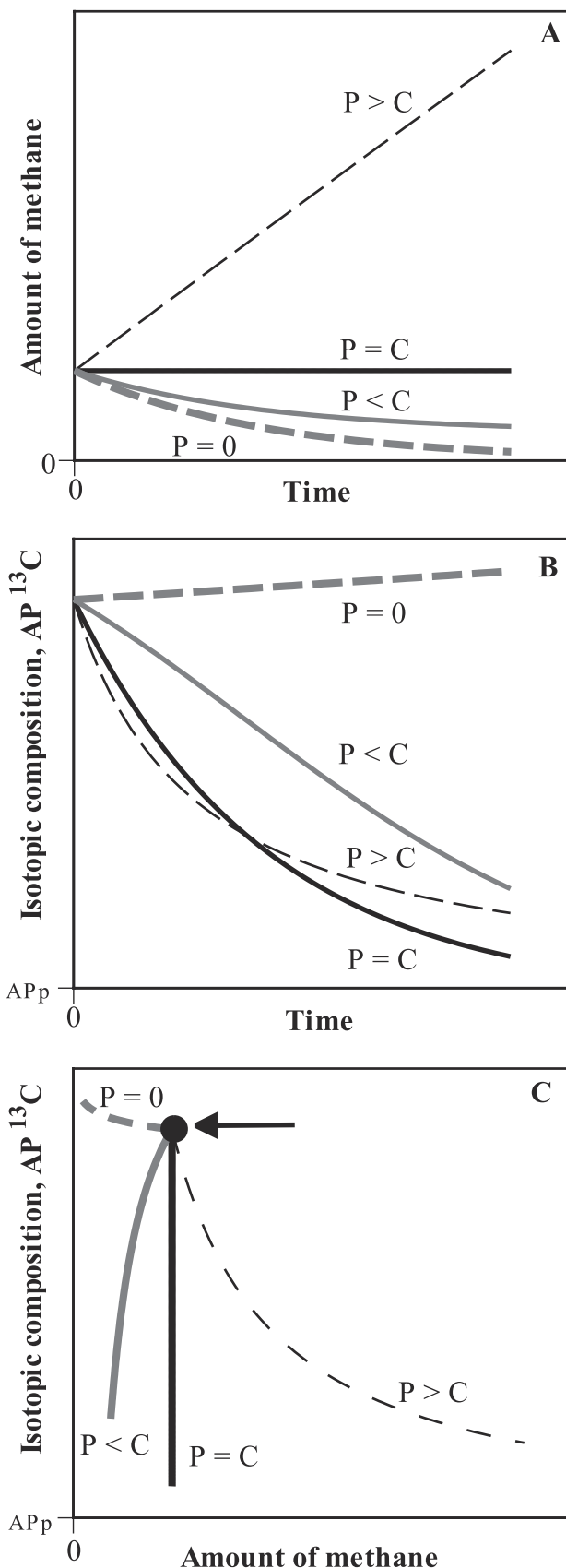
2.1. Dynamics of Unlabeled Methane

[8] We assume that the amount of methane present in the soil atmosphere (where the term “amount” refers to the number of moles of CH_4 in the closed system) is influenced solely by methane production and consumption. The balance between these two processes ultimately determines the net flux of methane between the soil and the atmosphere, described as

$$F = P - C, \quad (1)$$

where F is the net flux rate between the soil and the atmosphere (e.g., in units of moles per hour), P is the gross rate of methane production, and C is the gross rate of methane consumption.

[9] In the incubation chamber, methane concentrations can be expected to rise or fall over time in response to the balance between methane production and consumption. Because methane consumption follows Michaelis-Menten kinetics [Bender and Conrad, 1992; Roslev *et al.*, 1997], we can expect the rate of consumption to change with any changes in methane concentration over the course of the incubation. Atmospheric methane concentrations are typi-



cally below the K_m , so we can use a first-order relationship to model consumption [Fenchel *et al.*, 1998; King, 1997; Roslev *et al.*, 1997]. Thus

$$C_t = km_t, \quad (2)$$

where C_t is the instantaneous rate of methane consumption at time t , k is the first-order rate constant for consumption, and m_t is the amount of methane at time t . Because the number of moles is equivalent to concentration in a closed system of constant volume, we have modeled consumption in equation (2) as a first-order reaction with respect to the amount of methane, thus simplifying subsequent equations. The consumption constant, k , can be used to calculate the consumption rate at a particular methane concentration, b , (e.g., in units of microliters per liter) if k is corrected for the volume of the incubation container, v , and by the concentration of interest. Then

$$C = bkv. \quad (3)$$

Under most conditions, we can assume the methane concentration over the soil surface is equal to the atmospheric concentration of $1.8 \mu\text{L L}^{-1}$, so the gross consumption rate is calculated for $b = 1.8 \mu\text{L L}^{-1}$. Our formulation designates the atmospheric methane pool as the point of reference for measuring gross rates of methane production and consumption. Thus the derived constants (i.e., P , C , and k) reflect exchanges across the soil-atmosphere boundary, with the location of source/sink region defined empirically by the depth of label penetration into the soil.

[10] The consumption rate in equations (2) and (3) is expressed as a function of m and k . As a result, k incorporates environmental constraints, including oxygen limitation and other factors. Even though methane consumption might be a function of oxygen concentration at low oxygen conditions (i.e., $C = kO_2$) rather than a function of methane concentration (i.e., $C = kCH_4$), the practical determination of k according to equation (2) results in an empirically determined coefficient that incorporates effects due to both methane and oxygen.

[11] We can now incorporate equation (2) into equation (1) and represent instantaneous rates, like those in equation (2), as derivatives with respect to time:

$$F = \frac{dm}{dt} = P - km. \quad (4)$$

The solution of equation (4) is

$$m_t = \frac{P}{k} - \left(\frac{P}{k} - m_0 \right) \exp(-kt), \quad (5)$$

where m_0 is the initial mass of methane. The solution, m_t , describes how the amount of methane changes over time. These changes in mass can take on one of three qualitatively

Figure 2. (opposite) Qualitative dynamics of equations for (a) amount of methane over time, (b) isotope ratio over time, and (c) amount versus isotope ratio over time for combinations of production, P , and consumption, C , rates. In Figure 2b the isotopic composition in methane approaches AP_p , the isotopic composition of methane produced in the soil, for rates of $P > 0$. Arrows in Figure 2c indicate initial amount of methane and its isotopic composition.

different dynamics (Figure 2a): increasing ($P > C$), constant ($P = C$), or decreasing ($P < C$, $P = 0$).

[12] When both P and k are nonzero, the amount of methane in the system reaches steady state when

$$m = \frac{P}{k}. \quad (6)$$

This equilibrium point has been previously described for biogenic trace gases as the ‘‘compensation concentration’’ where productive and consumptive processes are balanced in the soil [Conrad, 1994].

2.2. Dynamics of Labeled Methane

[13] It is not possible to determine unique rates of production and consumption by only following changes in the amount of methane, because the single mass balance equation (4) depends on two unknown variables, P and k . However, by coupling the mass balance equation with an expression that describes how the ratio of labeled to unlabeled methane (i.e., the isotopic composition) changes over time, we are able to determine both P and k . While we describe the addition of ^{13}C methane, our treatment can be applied to other isotopes of methane like D/H or $^{14}\text{C}/^{12}\text{C}$.

[14] To uniquely follow the amount of ^{13}C label over time, we correct for any ^{13}C generated by methane production by subtracting the fixed isotopic composition of methane that is produced. The amount of added ^{13}C methane at time t can be related to the percent abundance of ^{13}C in total methane as

$$n_t = m_t(AP_t - AP_p), \quad (7)$$

where n_t is the amount of labeled methane, m_t is the total amount of methane, AP_t is the measured atom percent ^{13}C methane in the system, and AP_p is the atom percent ^{13}C of methane generated by methane production (see Appendix A for conventions of reporting isotopic composition).

[15] The equation used to model the total amount of methane (equation (4)) can be simplified and applied to reflect the amount of the labeled methane, n , following two modifications. First, because there is no production of labeled methane during incubation, we can remove the production term, P , from equation (4). Second, isotopic fractionation slows the rate of consumption of ^{13}C methane by a very slight but constant amount, α , as compared to unlabeled methane, which is overwhelmingly $^{12}\text{CH}_4$. The fractionation coefficient follows the notation: $\alpha = k_{13}/k_{12}$, where k_{12} is the first-order rate constant for consumption of $^{12}\text{CH}_4$ and k_{13} is the first-order rate constant for consumption of $^{13}\text{CH}_4$. The resulting equation describes the instantaneous change in the amount of label with respect to time as

$$\frac{dn}{dt} = -k\alpha n. \quad (8)$$

The solution to equation (8) describes how the mass of label changes over time:

$$n_t = n_0 \exp(-kat), \quad (9)$$

where n_0 is the initial mass of labeled methane.

[16] Having developed equations to describe the amount of both labeled and unlabeled methane, it now becomes

straightforward to describe how the isotopic composition of the system changes with time. The amount of methane and its isotopic composition are the two properties in the headspace that are measured during the incubation, and the equation for isotopic composition is necessary for calculating methane production.

2.3. Dynamics of Isotopic Composition

[17] We generate the equation for describing the isotopic composition over time by first rearranging equation (7) to the form

$$AP_t = \frac{n_t}{m_t} + AP_p. \quad (10)$$

Then, by defining m_t as in equation (5) and defining n_t as in equation (9), we get

$$AP_t = \left(\frac{n_0 \exp(-kat)}{\frac{P}{k} - \left(\frac{P}{k} - m_0\right) \exp(-kt)} \right) + AP_p. \quad (11)$$

[18] Equation (11) has two qualitatively different dynamics depending on the size of P with respect to C . When P is greater than C , equation (11) predicts a decline in the atom percent ^{13}C over time because production dilutes the labeled methane. Figure 2b demonstrates this behavior where, as time approaches infinity, the isotopic composition of methane, AP_t , approaches the isotopic composition of produced methane, AP_p , for all cases except where $P = 0$. In general, the rate at which AP_t approaches AP_p is greater when the combined rate of P and C (i.e., the turnover rate of the methane pool) is greater. When P is small as compared to C (illustrated for $P = 0$ in Figure 2b), methane in the system becomes enriched in ^{13}C , causing the isotope ratio to increase. This increase, known as a Rayleigh distillation [Hoefs, 1997], results from isotopic fractionation where the heavier isotope accumulates over time due to preferential consumption of $^{12}\text{CH}_4$ relative to $^{13}\text{CH}_4$.

[19] We have expressed the changes in methane amount and isotope ratio with respect to time (i.e., in equations (5) and (11)). However, the changes in amount can also be considered with respect to changes in the isotope ratio (Figure 2c) to observe the unique trajectory that is generated by each combination of production and consumption rates. As we describe in section 2.4, we use the product of methane amount and isotope ratio (i.e., n in equation (7)) to determine k , while we use the two measures separately (as in Figure 2c) to determine P .

2.4. Determination of Production and Consumption From Data

[20] The gross rates of methane production and consumption can be uniquely determined by fitting equations for the amount of labeled methane (equation (9)), the total amount of methane (equation (5) and the isotope ratio (equation (11))) to measured data. Figure 3 illustrates these principal equations and gives examples of their dynamics. We use a two-step process for fitting the equations to data. We first determine the consumption rate constant, k , by linear regression. Then we combine this value of k with measures of the amount of methane and its isotopic composition to determine P using a curve fitting routine.

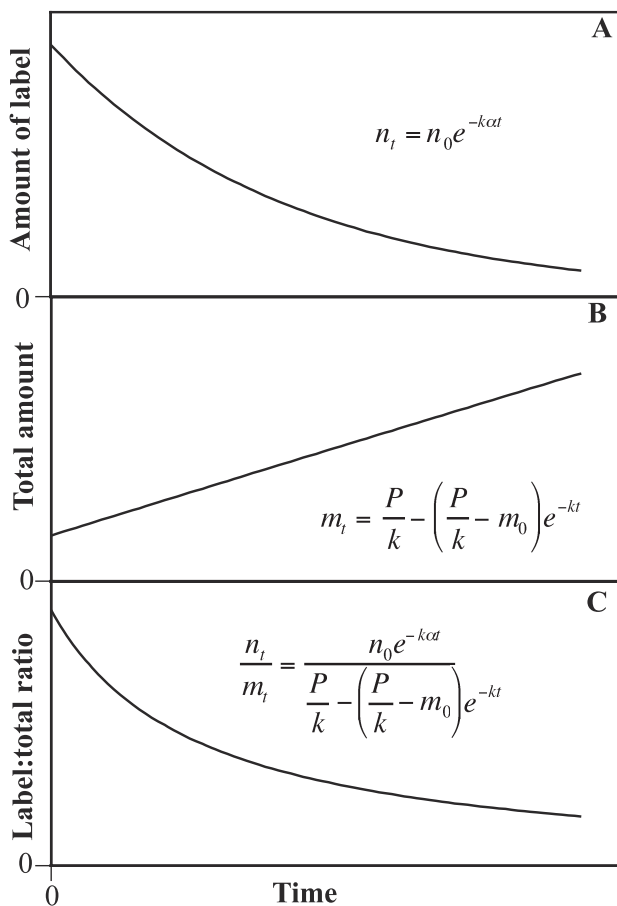


Figure 3. Fundamental equations used to calculate gross methane production and consumption presented with examples of their dynamics. (a) As we describe in section 2.4, the fit of the amount of labeled methane over time to equation (9) determines k . We then use this k and determine P as the best fit of data for both (b) the amount of methane to equation (5) and (c) the isotope ratio to equation (11).

[21] First, because equation (9) predicts a log linear relationship between the amount of label, n , and time, we log-transform n . We then calculate k as the slope of the linear regression of $\ln(n)$ versus time, multiplied by $1/\alpha$ to correct for fractionation against the labeled methane. From k , we calculate the gross methane consumption rate at atmospheric concentrations of methane (i.e., $1.8 \mu\text{L L}^{-1}$) using equation (3).

[22] In the second step, we calculate the gross production rate, P , by simultaneously fitting equation (5) for the amount of methane and fitting equation (11) for isotopic composition to measured data. From an initial amount and isotopic composition at $t = 0$, the combined effects of methane production and consumption drive the amount and isotopic composition of methane through one of four qualitatively different trajectories (Figure 2c). We calculate P recursively to find the best simultaneous fits of equations (5) and (11) to the measures of the amount and isotopic composition of methane during the incubation.

[23] To permit the recursive technique to fit amount and isotope data of different dynamic ranges and precisions, we

normalize the data using a “signal-to-noise” ratio that is analogous to the F ratio in analysis of variance [Neter *et al.*, 1990]:

$$N_{\text{AP}} = \frac{\text{SD}_{\text{obs-AP}}}{\text{SD}_{\text{prec-AP}}} \quad (12)$$

$$N_m = \frac{\text{SD}_{\text{obs-m}}}{\text{SD}_{\text{prec-m}}}, \quad (13)$$

where N_{AP} is the normalization factor for the isotope ratio, $\text{SD}_{\text{obs-AP}}$ is the observed standard deviation in atom percent ^{13}C during the incubation, and $\text{SD}_{\text{prec-AP}}$ is the analytical precision of isotopic determination expressed in standard deviations. Similarly, N_m is the normalization factor for the amount of methane, $\text{SD}_{\text{obs-m}}$ is the observed standard deviation in amount of methane during the incubation, and $\text{SD}_{\text{prec-m}}$ is the analytical precision for determination of the amount, expressed in standard deviations. These normalizing ratios have the effect of giving less weight to amount or isotopic data when changes in the measured data are small with respect to analytical precision.

[24] Through recursion, we minimize total error, E , between observed and expected values:

$$E = \left(\sum_{t=1}^j \frac{|\text{AP}_{\text{observed}}(t) - \text{AP}_{\text{expected}}(t)|}{\text{SD}_{\text{obs-AP}}} \right) N_{\text{AP}} + \left(\sum_{t=1}^j \frac{|m_{\text{observed}}(t) - m_{\text{expected}}(t)|}{\text{SD}_{\text{obs-m}}} \right) N_m, \quad (14)$$

where j is the number of observations made during the incubation. The net flux rate at atmospheric concentrations of methane can be calculated from equation (1) by subtracting the gross rate of consumption (C in equation (3)) from the gross rate of production, P .

3. Assumptions and Sensitivity Analysis

[25] Random errors in the analytical determination of methane amount or isotope ratio could potentially lead to systematic bias in estimated rates of methane production and consumption as a result of the nonlinearities in the model or the recursive curve fitting technique. To examine the potential for such effects, we performed a series of computer-simulated incubations, based on typical requirements for field incubations. In the computer simulations we generated incubation data for the amount of methane and the isotope ratios using equations (5) and (11), then added random, normally distributed analytical error to the data to simulate variance within the analytical precision. Finally, we analyzed the computer-generated data and calculated rates of methane production and consumption. In adding simulated variance, we used precisions typical for field incubations: $0.1 \mu\text{L L}^{-1}$ (1 SD) for determination of the amount of methane and 0.03 atom percent ^{13}C (1 SD, equivalent to 30‰) for stable isotope determination. To assess the effects of these errors across a range of methane production and consumption rates, we simulated combinations of low, medium, and high rates of methane production and consumption, giving nine combinations of P and k values. Each combination was simulated 500 times. We

Table 1. Results of Computer Simulation of Effects of Analytical Error on Calculated Methane Production, P , and First-Order Consumption Constant, k , Across Nine Combinations of Low, Medium, and High Rates of Methane Production and Consumption^a

Conditions	True k , L CH ₄ m ⁻² day ⁻¹	Estimated k , L CH ₄ m ⁻² day ⁻¹	True P , mg CH ₄ -C m ⁻² day ⁻¹	Estimated P , mg CH ₄ -C m ⁻² day ⁻¹
Low k , Low P	0	3 ± 165	0	0.002 ± 0.02
Low k , Med P	0	6 ± 170	0.25	0.24 ± 0.02
Low k , high P	0	6 ± 625	49	49 ± 2
Medium k , low P	807	834 ± 231	0	0 ± 0.01
Medium k , medium P	807	831 ± 231	0.25	0.25 ± 0.02
Medium k , high P	807	779 ± 624	49	49 ± 2
High k , low P	8066	8144 ± 1625	0	-0.006 ± 0.057
High k , medium P	8066	8219 ± 1623	0.25	0.245 ± 0.06
High k , high P	8066	8077 ± 719	49	49 ± 2

^aSimulated incubation data were generated from “known” rates using equations (5) and (11), analytical error was added to the data, and then P and k were calculated from the resulting data. Estimated values for P and k are averages and standard deviations from 500 simulated incubation.

optimized the length of incubations to ensure that the final methane concentrations remained above the field detection limit and the final isotopic compositions remained above natural abundance levels. For simulation, we used Microsoft Excel 2000 (Microsoft Corporation). The results of these simulations (Table 1) show that random analytical error does not induce significant bias in estimates of P and k ; average simulation values were always within 1 SD of true values. The results suggest that this technique is a consistent estimator of methane production and consumption.

[26] Having established the robustness of the model to random analytical errors, we now consider its sensitivity to violations of the underlying assumptions, beginning with the instantaneous fractionation rate during methane consumption, α . *Snover and Quay* [2000] reviewed published values for α and reported a range between 0.984 and 0.973 for pure cultures of methane-consuming bacteria. From this range, we chose an assumed fractionation rate of 0.98. We then examined the sensitivity of calculated consumption and production rates to any departure from this assumed fractionation rate by incubated soils. We used additional computer-simulated incubations to quantify the sensitivity of P and k to differences between “assumed” and “true” fractionation rates by varying the true fractionation rate and analyzing the data using our assumed fractionation rate. By varying the true α between 1 and 0.9 in simulations using the nine combinations of P and k listed in Table 1, we found that underestimating the true fractionation rate caused both P and k to be underestimated. Conversely, overestimating the fractionation rate caused both P and k to be overestimated. Despite this potential for error, the magnitude of this effect is small for the range of k and P studied, generating ~1% error in both P and k for every 1% error in α . The worst-case scenario in our simulations (true $P = 0$ mg CH₄-C m⁻² day⁻¹, true $k = 8000$ L CH₄ m⁻² day⁻¹, true $\alpha = 1$ and assumed $\alpha = 0.98$) resulted in a calculated $P = 0.089 \pm 0.05$ (1 SD). The magnitude of this error is near the detection limit for the method, as quantified from field incubations that do not contain any soil (termed “field controls” below). We conclude that within biologically plausible ranges, errors in our assumed rates of isotopic fractionation are not likely to induce considerable bias in estimates of P and k .

[27] Our model assumes a known and constant isotopic composition, AP_p , of the methane produced in the soil. The

sensitivity of the model to this assumption depends on the initial amount of isotopic enrichment and the extent of isotopic dilution that occurs during the incubation. We have assumed the $\delta^{13}\text{C}$ of methane produced by methanogens to be -60‰ (1.05 atom percent ¹³C), a commonly observed, intermediate value within the observed range of -50 to -100‰ [*Whiticar*, 1993]. At high enrichment levels, deviation from the assumed value within the observed range generates an error of approximately the same size as analytical error and is thus not important. However, the error can become larger when turnover of the methane pool drives the isotope ratio down to levels that are near natural abundance. Very small differences between the measured isotopic composition, AP_p , and the assumed value for AP_p near the end of an incubation can exert large leverage on the regression for calculating k . This problem can be avoided by using sufficient initial isotopic enrichment of the methane pool and by ending the incubation before the enrichment falls to near-natural abundance levels.

[28] Violations of assumptions about the dynamics of the amount of methane are unlikely to lead to biased results. Our model calculates methane production over the entire incubation period (yielding an average rate) and therefore averages out any finer grained temporal variations that may occur in production rates. As a result, information about nonconstant rates is lost, but no artifacts are created. Any violation of assumptions about the first-order consumption of methane would introduce nonlinearity in the otherwise linear relationship between the log of label mass, n , and time and can therefore be examined empirically.

4. Field Application of Technique and Lab Methods

4.1. Field Sites and Techniques

[29] To assess the general applicability of this technique, we measured methane dynamics for soils located in Hawaii and in upstate New York. In order to sample soils that ranged widely in methane production and consumption rates, we selected three naturally formed gradients in soil moisture. The first two were along orographic precipitation gradients in montane tropical forests on the Hawaiian Islands of Maui and Kauai, and the latter gradient was a topographic cline from forest upland to riparian wetland in

New York State. Both the Maui and Kauai gradients are dominated by one of two native tree species: *Acacia koa*, which is only present in the drier two sites of each gradient, and *Meterosideros polymorpha*, which is present on most sites in both gradients but dominant only on the wetter sites. Soils on both gradients are derived from volcanic shield material, ~500,000 years old on the Maui gradient and ~4,100,000 years old on the Kauai gradient. Soil carbon content on these gradients ranges from 9% (weight/weight percent) in the dry sites to 46% in the wet sites. We did not encounter standing water in any site along these gradients. Sites along the Maui gradient have been described in detail by *Schuur et al.* [2001].

[30] The topographic cline in New York consisted of mixed maple and oak (*Acer* spp., *Quercus* spp.) woodland on the most well-drained site, sedge (*Carex* spp.) in the intermediate moisture sites, and an unvegetated stream sediment at the wet end. Soils in this part of New York State are derived from shale and are generally high in clay. Along this gradient, the soils increased in carbon content with soil moisture, from 4% in the upland to 33% in the wettest site. Standing water was only present on the wettest site. In addition to this topographic gradient, we also sampled two contrasting sites in a hemlock (*Tsuga canadensis*) forest in New York State: one on well-drained and one on poorly drained soils. Like the other upstate New York sites, the soils at these hemlock sites were derived from shale, but the mineral soils were overlain with a thick organic horizon, >8 cm in the drier site and >30 cm in the wet site. At all sites in this study, we sampled soils where soil moisture was uniform with depth as opposed to soils where a well-drained horizon may overlay a waterlogged horizon.

[31] We performed short-term (3–6 hours) incubations of intact soil cores at each site. We carefully collected undisturbed soil samples of the top 10–15 cm of soil with a corer that contained a plastic sleeve (15 cm deep, 5 cm diameter). Keeping the soil core within the sleeve, we then sealed the bottom end of the core with a plastic cap to eliminate gas exchange from soil surfaces that would not have been exposed to the atmosphere. The soil was sealed into a 1-quart canning jar to create a closed system for the $^{13}\text{CH}_4$ additions; the lid of the jar had been fitted with a port for gas sampling. We incubated soils immediately by burying the jar vertically in the soil near where the sample had been taken. Temperature and light therefore remained very similar to original conditions.

[32] We enriched the atmosphere in the incubation jar by adding labeled methane at the beginning of the incubation. Our target was an isotopic enrichment of 2–10 atom percent ^{13}C -methane. This addition led to a 2–10% increase in the headspace methane concentration so that, for example, a 5 atom percent addition to an incubation at atmospheric concentration would yield an increase from 1.80 to 1.89 $\mu\text{L CH}_4 \text{ L}^{-1}$. The isotopically enriched methane was diluted with air from 99% $^{13}\text{CH}_4$ (Isotec, Inc.) prior to its addition to the incubation containers. To ensure even initial distribution of the label, we immediately mixed the atmosphere of the incubation jar five times with a 60-mL syringe and left the incubation jar to

preincubate for 30–45 min so that the rapid, diffusive redistribution of the isotope into the soil core would not bias our measures of isotope dynamics [see *Andersen et al.*, 1998].

[33] To adequately follow changes in methane mass and isotopic composition over the course of the incubation, we collected at least four samples: one sample after the preincubation ($t = 0$) and three samples spaced at roughly equal intervals throughout the remainder of the incubation. Typical headspace volumes were ~800 mL, while sample volumes were 60 mL. We added a known volume of ultrahigh-purity helium to the incubation jar following each sample removal to prevent any effects due to pressure variations; all measures of methane concentrations were corrected for this helium addition. Occasionally, samples of either methane concentration or isotope ratio were lost due to analytical or other errors. In such cases, no data was used for that time point toward the calculation of methane production and consumption rates.

[34] Concurrent with each set of soil incubations, we incubated a jar without a soil core as a field control to test for leakage or any other effect not due to the soils. These controls also served as tests of analytical precision. The variance in measured amounts and isotope ratios of methane in these controls was used in the error calculation (equations (12) and (13)) for determining methane production rate. To test for any abiotic soil effects on methane mass and isotope ratio, we also performed a laboratory experiment using soil samples that had been autoclaved at 250°C for 90 min at a pressure of 140 kPa.

[35] We stored and transported gas samples in glass serum vials with aluminum crimp tops, fitted with 20-mm butyl rubber septa (Geomicrobial Inject Technologies, Oechelata, Oklahoma). Compared with other types of septa, we found that these exhibited minimum leakage and minimum blank contamination. We divided each 60-mL gas sample from the incubation into two parts; 10 mL for gas chromatographic analysis were compressed into 5-mL vials that had previously been evacuated, and the remaining 50 mL were compressed into 60-mL vials that had previously been flushed with ultrahigh-purity helium. To account for the small amount of leakage and/or the presence of blanks that can arise from the storage and transport of samples, we filled vials in the field with known standards and corrected the concentration of the samples for any consistent changes in the standards. The correction for 5-mL vials typically included subtraction of a blank of ~0.4 $\mu\text{L L}^{-1}$ and accounting for ~7% leakage. The larger 60-mL vials used for isotopic analysis had trivial blanks and leakage, so no correction was applied. We analyzed the 5-mL vials for methane concentration within 1 week of sampling and analyzed the 60-mL vials within 3 weeks.

4.2. Laboratory Techniques

[36] We determined the methane concentration by gas chromatography on an SRI 8610 with a Hayesep N column or on a Varian 3400 cx with a Chromosorb 102 column. Typical standard deviations for repeated measurement of standard air was <0.1 $\mu\text{L L}^{-1}$. Gas chromatographs were calibrated by analyzing standards of at least three levels of

methane in triplicate and calculating the average instrument response for each standard. No methane peak was ever present in methane-free gases, so only the instrument response (i.e., slope) was used. The detection limit for methane was $0.1 \mu\text{L L}^{-1}$, and all measured concentrations below that limit are reported as $0.05 \mu\text{L L}^{-1}$.

[37] Methane was prepared for isotopic analysis on a highly modified Europa Scientific ANCA TG, similar to systems described by *Chanton et al.* [1992] and *Brand* [1995]. In our system an air sample was manually introduced and carried by ultrahigh-purity helium under a pressure of 120 kPa. The gas stream passed through a chemical and a cryogenic trap to remove water vapor, carbon dioxide, and carbon monoxide: $\text{Mg}(\text{ClO}_4)_2$ removed water vapor, Schutze Reagent (LECO Corporation) oxidized CO to CO_2 , Carbosorb (a NaOH-based compound, PDZ Europa) removed CO_2 , and a liquid nitrogen trap removed any remaining CO_2 water vapor and other condensable gases. Following purification the sample methane was oxidized to CO_2 in an oven at 1050°C over a nickel and platinum catalyst. Water produced during combustion was removed in an isopropanol-dry ice mixture cryogenic trap maintained at $-40^\circ\text{C} \pm 5^\circ\text{C}$. The sample CO_2 was cryofocused in a coil of nickel tubing immersed in liquid nitrogen and was subsequently transferred to the mass spectrometer, where an open split admitted a fraction of the sample CO_2 to the ion source. Isotopic analysis was performed on a Europa Scientific Geo 20–20 stable isotope ratio mass spectrometer (PDZ Europa) calibrated to a working standard of air containing $2 \mu\text{L L}^{-1}$ methane (4.5 nmol CH_4 per 50 mL sample), $\delta^{13}\text{C} = -40.95\text{‰}$ as calibrated from the natural gas standard (NGS1). Typical analytical reproducibility of standards was $\pm 1\text{‰}$ (1 SD).

[38] We evaluated performance of the mass spectrometer and inlet system in several different ways. Most importantly, we observed no effect of contaminants or of changing sample size on the measured isotope ratio of methane. Injection of ultrahigh-purity helium produced very small system blanks, typically ~ 0.2 nmol. Samples were corrected for this blank. Experimentally elevated concentrations of carbon dioxide, an important potential contaminant, did not affect the isotope ratio of standards. Replicate samples of air containing ambient CO_2 (~ 355 ppm, $\delta^{13}\text{C}$ of CO_2 approximately -7‰) and elevated CO_2 (33,000 ppm, $\delta^{13}\text{C}$ of CO_2 $\sim 0\text{‰}$) had no effect on the measured $\delta^{13}\text{C}$ of $\text{CH}_4\text{-C}$ ($p > 0.4$, $n = 2$). Typically, there was very little carryover from one sample to the next, and the carryover affected only samples of vastly different mass and isotopic composition. We avoided side-by-side analyses of such different samples and applied an empirically determined carryover rate that was typically $\sim 0.5\%$. Although isotope ratios may vary as a function of sample size in some mass spectrometer systems (N. Ostrom and S. Prossor, personal communication, 1998), we observed no effect $> 5\text{‰}$ across $10\times$ variation in sample mass in our frequent tests of such linearity.

[39] We analyzed soils in all sites for moisture content by drying 24 hours at 105°C . We adopted soil particle densities for mineral and organic soils (2.65 and 1.4 g cm^{-3} ,

respectively) from *Culley* [2000] and calculated percent water-filled pore space from gravimetric water content and particle density. All basic data analysis and recursive analyses were performed in Microsoft Excel 2000. All other statistics were calculated in JMP (SAS Institute, Inc.).

5. Field Results

[40] Here we present results from 175 incubations, including 130 field-incubated soil cores from 17 sites. The model fit to measured data was very strong for the vast majority of soils encountered in this study. The median coefficient of determination, r^2 , between observed and model data points was 0.94 for the fit of data on the amount of methane with equation (5) (104 of 130 incubations had r^2 values above 0.5) and was 0.90 for the fit isotope ratio data with equation (11) (98 of 130 incubations had r^2 values above 0.5). The r^2 values were higher when changes in mass or isotopic composition were higher ($p < 0.003$ for both mass and isotope data); the strength of fit was therefore greatest in soils that were more metabolically active.

[41] To illustrate typical data and the model fit, we show the changes in the amount of labeled methane over time (Figures 4a and 4b) and the changes in the amount and isotope ratio of methane (Figures 4c and 4d) for two soil incubations: one with negative net flux (gross consumption $>$ gross production) and one with positive flux (gross production $>$ gross consumption). For the soil with net negative flux (net consumption of $5.2 \text{ mg CH}_4\text{-C m}^{-2} \text{ day}^{-1}$), we determine k from the data in Figure 4a and calculate a gross consumption rate of $5.4 \text{ mg CH}_4\text{-C m}^{-2} \text{ day}^{-1}$. The existence of methane production is demonstrated qualitatively by a decline in the methane isotope ratio over the course of sampling (Figure 4c). We fit equation (11) to this isotope decline and fit equation (5) to the data for the amount of methane ($r^2 = 0.99$ for fit of equation (11) to isotope data, 0.99 for fit of equation (15) to amount data) and calculate a gross production rate of $0.18 \text{ mg CH}_4\text{-C m}^{-2} \text{ day}^{-1}$. This incubation illustrated that both productive and consumptive processes co-occurred in this soil, even though traditional measures of atmosphere-soil methane flux indicated net consumption.

[42] In contrast, we show in Figures 4b and 4d a soil that displayed positive methane flux (i.e., net production, $25.4 \text{ mg CH}_4\text{-C m}^{-2} \text{ day}^{-1}$). In this case, the fit for the amount of labeled methane versus time (Figure 4b) leads to a gross consumption rate of $1.1 \text{ mg CH}_4\text{-C m}^{-2} \text{ day}^{-1}$. Our model fit to the plot of the amount of methane and its isotope ratio (Figure 4d; $r^2 = 0.98$ for fit of equation (5) to amount data, $r^2 = 0.99$ for fit of equation (11) to isotope data) reveal a gross methane production rate of $26.5 \text{ mg CH}_4\text{-C m}^{-2} \text{ day}^{-1}$. In this case, the gross methane consumption rate was considerably less than the gross methane production rate, despite the elevated abundance of methane resulting from methane production.

[43] We used empty incubation containers and sterilized soils to determine if trends in the amount of methane and its isotopic composition can occur in the absence of live soils and to establish a method detection limit. Our tests showed that statistically significant rates of methane pro-

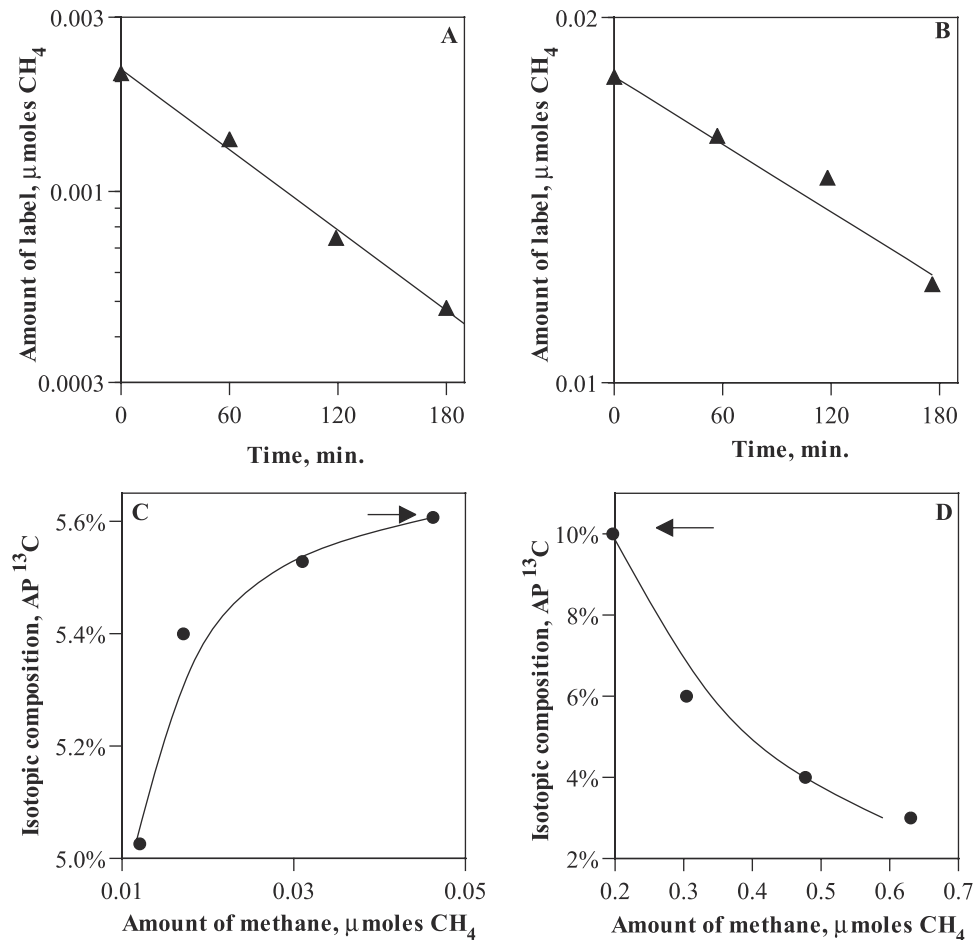


Figure 4. (a, b) Changes in amount of labeled methane as a function of time and (c, d) changes in total amount and isotopic composition of methane for field-incubated soils. Symbols mark measured values, while lines are model fits. In Figures 4a and 4b the model fit is for equation (9) to the data, while in Figures 4c and 4d the model fit is for equations (5) and (11) to the data. Note the log scale on the y axis of Figures 4a and 4b. Arrows identify initial amount of methane and its isotopic composition for incubation. Figures 4a and 4c show measured and model trends for a forest soil from a Hawaiian site with negative methane flux ($P < C$). Figures 4b and 4d show those trends for a soil sample from a wetland site in New York State with positive methane flux ($P > C$).

duction and consumption only occurred in the presence of live soil (test for production and consumption >0 : $p < 0.001$ in live soil treatment, $p > 0.22$ for autoclaved soil and no soil treatments, $n = 4$ for each treatment). Similarly, empty containers that were incubated to serve as controls in the field displayed rates of methane production and consumption not different from zero ($p > 0.9$ for both production and consumption). We adopted the average rates of gross production ($0.04 \text{ mg CH}_4\text{-C m}^{-2} \text{ day}^{-1}$) and consumption ($0.11 \text{ mg CH}_4\text{-C m}^{-2} \text{ day}^{-1}$) from the field controls as the minimum detection limit for measurement in the field.

[44] Our 130 field incubated soils displayed a wide range of net methane flux rates, from -8.9 to $926 \text{ mg CH}_4\text{-C m}^{-2} \text{ day}^{-1}$. In Figure 5 we show the contributions of gross methane production and consumption to the net flux rate, and we partition the range of net fluxes into three categories: those with positive net flux ($>0.2 \text{ mg CH}_4\text{-C m}^{-2}$

day^{-1}), negative net flux ($<-0.2 \text{ mg CH}_4\text{-C m}^{-2} \text{ day}^{-1}$), and near zero net flux (between 0.2 and $-0.2 \text{ mg CH}_4\text{-C m}^{-2} \text{ day}^{-1}$). We observed gross rates of methane production across more than 4 orders of magnitude (0.04 – $930 \text{ mg CH}_4\text{-C m}^{-2} \text{ day}^{-1}$), while methane consumption varied across a much smaller range (0.11 – $9.2 \text{ mg CH}_4\text{-C m}^{-2} \text{ day}^{-1}$). Occasionally, we measured small, negative production and consumption rates that are biologically meaningless but arise from analytical error when rates of the process are very low. These data are included here to illustrate the situations where they can arise and because elimination of such points can induce bias.

[45] Comparisons within net flux categories (i.e., within columns of Figure 5) provide information about the interaction between gross production and consumption rates. Soils with negative net flux had only low rates of gross methane production ($<0.5 \text{ mg CH}_4\text{-C m}^{-2} \text{ day}^{-1}$), but rates of gross methane consumption in these soils ranged from

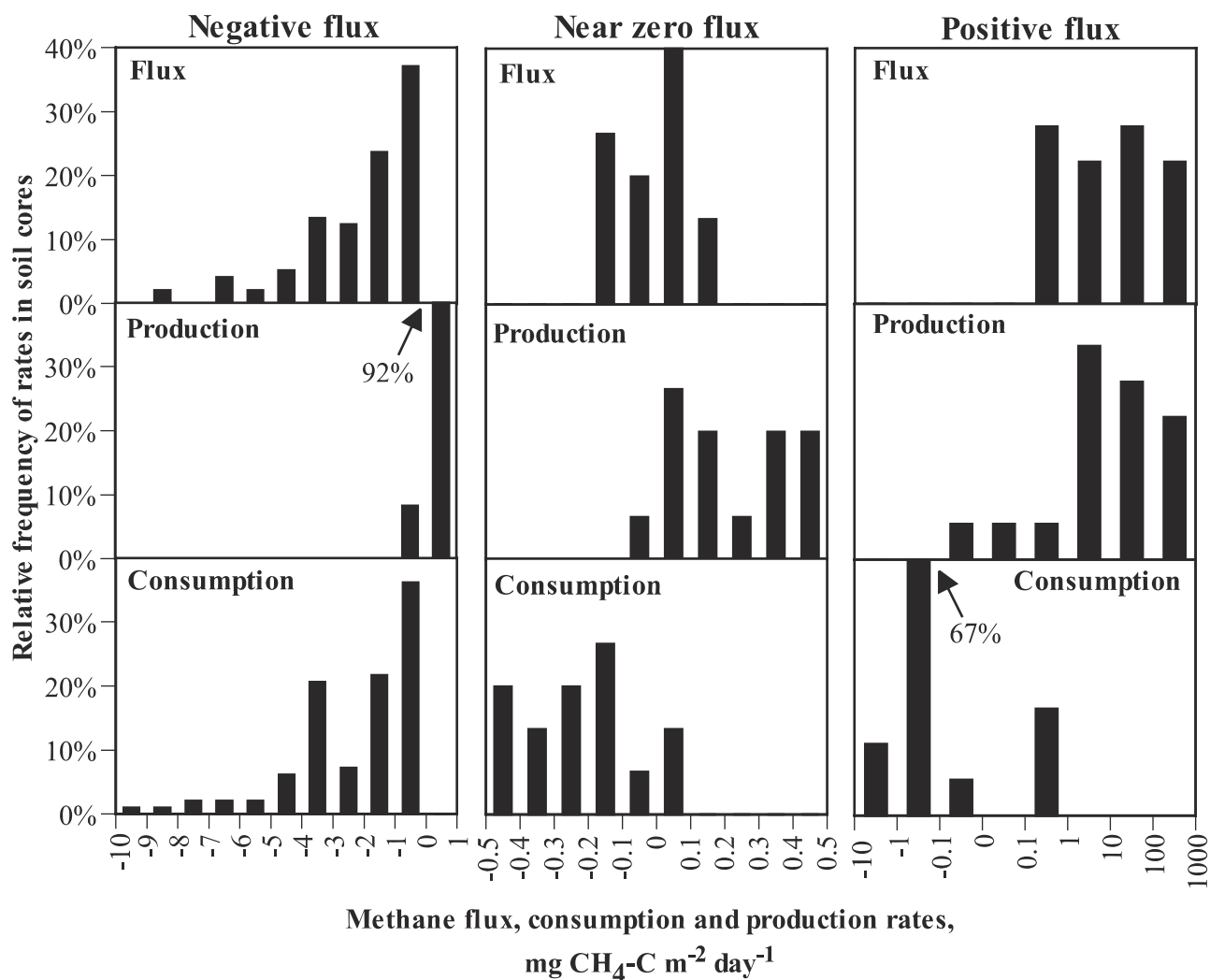


Figure 5. Frequency histograms of methane production, consumption, and flux for 130 incubated soil samples from 17 field sites. The y axis for all graphs is relative frequency at which a particular rate was observed. Methane consumption rates are assigned negative values to indicate their effect on methane flux. Note that bins along x axes for negative and near-zero fluxes are on a linear scale, while bins along the x axis of positive flux follow a nonlinear scale. A total of 97 samples had negative net flux, 15 were near zero, and 18 had positive methane flux.

near zero to the largest observed consumption rates. While near-zero flux could occur at any rate of equal production and consumption (i.e., $P = C$), we found only low rates of production and consumption. Soils with net positive flux had a very wide range of gross production rates, including the largest observed rate ($930 \text{ mg CH}_4\text{-C m}^{-2} \text{ day}^{-1}$) opposed by only very low rates of consumption; only one sample had rates of consumption in excess of $2 \text{ mg CH}_4\text{-C m}^{-2} \text{ day}^{-1}$.

[46] Comparisons across flux categories (i.e., within rows of Figure 5) provide information about how gross rates of production and consumption correspond to net flux. The primary difference between soils with negative net flux and soils with near-zero net flux is the absence of high rates of gross methane consumption. In contrast, the difference between soils with near-zero flux and those with positive flux is the presence of very high rates of methane produc-

tion (50% are above $10 \text{ mg CH}_4\text{-C m}^{-2} \text{ day}^{-1}$). Surprisingly, the greater range and more uniform distribution of positive net flux rates appeared despite a much smaller sample size ($n = 18$) as compared to soils with negative net flux ($n = 97$).

[47] One of our most interesting results is the common occurrence of gross methane production in soils with negative net flux. The rates of gross methane production in these soils are small ($0.15 \pm 0.15 \text{ mg CH}_4\text{-C m}^{-2} \text{ day}^{-1}$, mean ± 1 SD, $n = 97$), but they are significantly greater than the methane production rates observed for controls ($p < 0.0001$, $n = 33$ controls, $n = 97$ soils), and the rates are greater than expected from violation of assumptions.

[48] As expected from previous observations and theories on the metabolic constraints of methane production and consumption, the differences in the methane flux rate are associated with variation in soil moisture (Figure 6). Soils

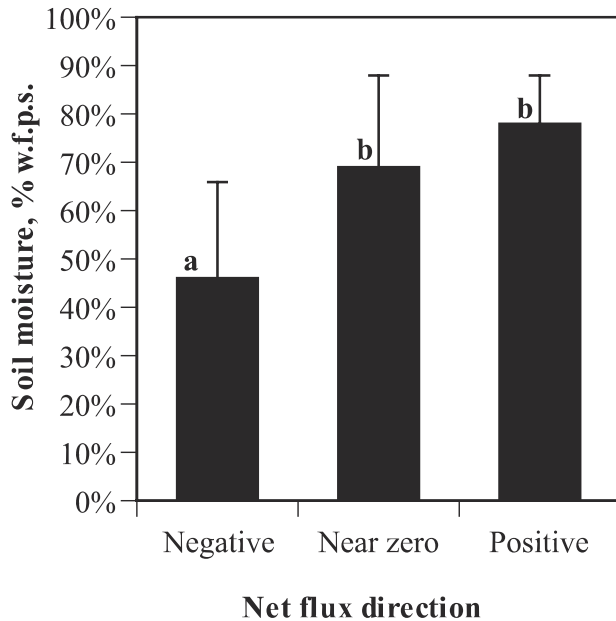


Figure 6. Soil moisture levels (percent water-filled pore spaces) for incubated soils with negative methane flux, near-zero flux, and positive flux. Error bars are 1 standard deviation. Letters (a versus b) denote group means that are not statistically different.

with negative flux generally were significantly drier ($p < 0.001$), while wetter soils had near-zero or positive net methane flux. This relationship is discussed in greater detail by J.C. von Fischer and L.O. Hedin (manuscript in preparation, 2002).

6. Discussion

[49] It has been almost 50 years since *Kirkham and Bartholomew* [1954, 1955] described a method for determining gross rates of nitrogen transformations in soils using additions of the stable isotope, ^{15}N . Application of their pool dilution approach has brought tremendous insight into the processing of nitrogen in soils [e.g., *Davidson et al.*, 1993; *Hart et al.*, 1997; *Stark and Hart*, 1997; *Currie et al.*, 1999; *Neill et al.*, 1999; *Perakis and Hedin*, 2001]. Here we have extended the principles of stable isotope pool dilution to the study of methane production and consumption using additions of ^{13}C methane, although we recognize that other trace gases (e.g., nitrous oxide, carbon monoxide, and methyl halides) may be amenable to similar study.

[50] The strong fit (high r^2 values) between our model and the measured changes in the amount of methane and its isotope ratio support the idea that the model has captured the essential features for measuring methane production and consumption. Further, the absence of measured production and consumption in incubations that lack biology suggests that the overall technique is not subject to nonbiological artifacts. From these field results and the results of the sensitivity analysis, we conclude that the technique is an accurate method for determining gross rates of methane production and consumption. In addition, the detection

limits for measuring methane production and consumption are very low as compared to the range of biologically possible rates (e.g., *Bubier and Moore* [1994] and this study). The sensitivity could be improved through longer incubations, although the improved sensitivity would come at the risk of inducing changes in the soil microbial community [*Madsen*, 1998]. The results presented here illustrate the potential of this technique for studying the controls on methane flux from soils. A fundamental question for understanding methane flux lies in knowing which combinations of production and consumption rates occur most frequently. In soils with negative flux, we observed consistently low production rates coupled with a relatively wide range of consumption rates, while high and extremely wide variation in production rates were coupled with lower consumption rates at positive flux. These data support the idea that high rates of production and high rates of consumption are mutually exclusive. An alternative hypothesis that was not supported by our data is that high rates of methane production and consumption can co-occur and lead to near-zero methane flux.

[51] One insight gained by recognizing the relationship between methane production, consumption, and flux, identified by *Matthews and others* [*Matthews*, 2000, and references therein], is the knowledge that regulators of methane flux, like soil moisture, may control both production and consumption. Our measures of soil moisture support the idea that wetter soils have lower methane consumption but do not necessarily have higher rates of production. Future application of this technique can be used to link gross rates of consumption, production, and flux with each other and with gas diffusion and other environmental controls.

[52] Our results also have implications for understanding soil microbial ecology. We observed measurable rates of methane production in soils with net negative flux. The archaeobacteria considered the true methanogens are strict anaerobes [*Zinder*, 1993]. It is therefore counterintuitive that methane production should occur in oxic soils, given the strictly anaerobic requirements of the organisms. Previously, *Andersen et al.* [1998] measured methane production of a similar rate in an oxic soil ($0.1 \text{ mg CH}_4\text{-C m}^{-2} \text{ day}^{-1}$ as compared to the $0.15 \text{ mg CH}_4\text{-C m}^{-2} \text{ day}^{-1}$ measured here) and attributed it to methane-producing archaeobacteria, based on fluorescence microscopy. These observations support the idea that anoxic microsites are present and biogeochemically active within oxic soils. Microbial activity within anoxic microsites has been hypothesized to occur, based on the presence of anaerobic organisms in oxic soils [*Peters and Conrad*, 1995] and on the propensity for oxic soils to produce methane rapidly when placed under anoxic conditions [*Yavitt et al.*, 1995] and from oxygen microprobes [*Sexstone et al.*, 1985]. However, *Rimbault et al.* [1988] have measured extremely low rates of methane production resulting as a metabolic byproduct in the eubacteria, *Clostridia*. On the basis of the potential for nonmethanogenic organisms to produce trace quantities of methane, it seems premature to assume that methanogens, alone, are responsible for production of methane in oxic soils.

[53] The presence of active methane production in negative flux soils does offer a potential explanation for why

incubated soil samples cannot reduce methane concentrations to that which is expected based on the enzymatic capacity of known methanotrophs [Conrad, 1993]. We offer the testable, alternate hypothesis that methane production, something that we measured commonly in dry soils, would create a compensation concentration [Conrad, 1994] that may be responsible for the apparent threshold. Similarly, hidden methane production may also be responsible for the generally lower rates of isotopic fractionation that have been measured for soils as compared to pure cultures of methanotrophs [Snover and Quay, 2000]. Perhaps the very low rates of methane production can provide an important source of energy for methane consumers.

Appendix A: Conventions for Reporting Isotopic Composition

[54] The relative abundance of stable isotopes is commonly reported in one of three notations.

1. The first notation gives the ratio of heavy to light isotopes, $R = {}^{13}\text{C}/{}^{12}\text{C}$. This ratio is a "raw" measure made by isotope ratio mass spectrometers.

2. The second notation gives the atom percent of the heavy isotope, AP = $({}^{13}\text{C}/({}^{12}\text{C}+{}^{13}\text{C})100$). Atom percent excess, or APE, expresses the relative abundance of the heavy isotope above natural abundance levels. APE is calculated as the AP of an isotopically enriched material minus the AP at natural abundance levels of enrichment.

3. The third notation is the delta notation, $\delta^{13}\text{C} = ((R_s - R_a)/R_a)1000$, where R_s is the isotope ratio of the sample and R_a is the isotope ratio of a standard. This notation is often used to highlight small differences in isotopic composition that occur near natural abundance enrichments.

Notation

α	fractionation factor for methane consumption.
AP_p	atom percent ${}^{13}\text{C}$ of methane produced in the soil.
AP_t	atom percent ${}^{13}\text{C}$ of methane at time t .
b	concentration of methane in the atmosphere.
C, C_t	rate of methane consumption.
E	sum of normalized error between observed and expected values.
k	first-order constant for methane production.
m, m_t	total amount of methane or the amount at time t .
m_0	total amount of methane at $t = 0$.
n, n_t	amount of labeled methane or the amount at time t .
n_0	amount of labeled methane at $t = 0$.
P	rate of methane production.
$\text{SD}_{\text{obs-AP}}$	observed variance in AP_t over the course of the incubation, in standard deviations.
$\text{SD}_{\text{obs-m}}$	observed variance in the amount of methane over the course of the incubation, in standard deviations.
$\text{SD}_{\text{prec-AP}}$	precision, or observed variance in AP_t in field controls, in standard deviations.
$\text{SD}_{\text{prec-m}}$	precision, or observed variance in the amount

of methane in field controls, in standard deviations.

N_{AP}	normalization factor for isotopic composition data.
N_m	normalization factor for data on the amount of methane.
t	time.
v	volume of air in the incubation chamber.

[55] **Acknowledgments.** This work was supported by grants from the Andrew W. Mellon Foundation, a National Science Foundation Research Training grant graduate fellowship, and a National Aeronautics and Space Administration Earth System Science graduate fellowship. We thank Lou Derry, Nathaniel Ostrom, and Todd Walter for their help and advice and thank Jonathan Comstock and Jim Burdett in the Cornell Boyce Thompson Stable Isotope Lab for their generous support. We thank Pamela Matson, Ted Schuur, and Peter Vitousek for invaluable comments and assistance with access to field sites. We thank Herald Farrington and several others for their assistance in the field. Finally, we thank Jeff Chanton and two anonymous reviewers who provided valuable criticism on this manuscript.

References

- Andersen, B. L., G. Bidoglio, A. Lejp, and D. Rembges, A new method to study simultaneous methane oxidation and methane production in soils, *Global Biogeochem. Cycles*, 12(4), 587–594, 1998.
- Bender, M., and R. Conrad, Kinetics of CH_4 oxidation in oxic soils exposed to ambient air or high CH_4 mixing ratios, *FEMS Microbiol. Ecol.*, 101, 261–270, 1992.
- Brand, W. A., Precon: A fully automated interface for the pre-GC concentration of trace gases in air for isotopic analysis, *Isot. Environ. Health Stud.*, 31, 277–284, 1995.
- Bubier, J. L., and T. R. Moore, An ecological perspective on methane emissions from northern wetlands, *Trends Ecol. Evol.*, 9(12), 460–464, 1994.
- Chanton, J. P., G. J. Whiting, W. Showers, and P. Crill, Methane flux from Paltandra virginica: Stable isotope tracing and chamber effects, *Global Biogeochem. Cycles*, 6(1), 15–33, 1992.
- Chanton, J. P., G. J. Whiting, N. E. Blair, C. W. Lindau, and P. K. Bollich, Methane emission from rice: Stable isotopes, diurnal variations, and CO_2 exchanges, *Global Biogeochem. Cycles*, 11(1), 15–27, 1997.
- Cicerone, R. J., and R. S. Oremland, Biogeochemical aspects of atmospheric methane, *Global Biogeochem. Cycles*, 2(4), 299–327, 1988.
- Conrad, R., Mechanisms controlling methane emission from wetland rice fields, in *The Biogeochemistry of Global Change: Radiative Trace Gases*, edited by R. S. Oremland, pp. 317–335, Chapman and Hall, New York, 1993.
- Conrad, R., Compensation concentration as critical variable for regulating the flux of trace gases between soil and atmosphere, *Biogeochemistry*, 27, 155–170, 1994.
- Culley, J. L. B., Density and Compressibility, in *Soil Sampling and Methods of Analysis*, edited by M. R. Carter, pp. 529–539, CRC Press, Boca Raton, Fla., 2000.
- Currie, W. S., K. J. Nadelhoffer, and J. D. Aber, Soil detrital processes controlling the movement of N-15 tracers to forest vegetation, *Ecol. Appl.*, 9(1), 87–102, 1999.
- Davidson, E. A., and J. P. Schimel, Microbial processes of production and consumption of nitric oxide, nitrous oxide and methane, in *Biogenic Trace Gases: Measuring Emissions From Soil and Water*, edited by P. A. Matson and R. C. Harriss, pp. 327–357, Blackwell Sci., Malden, Mass., 1995.
- Davidson, E. A., P. A. Matson, P. M. Vitousek, R. Riley, K. Dunkin, G. Garcia-mendez, and J. M. Maass, Processes regulating soil emissions of NO and N_2O in a seasonally dry tropical forest, *Ecology*, 74(1), 130–139, 1993.
- Etheridge, D. M., G. I. Pearman, and P. J. Fraser, Changes in tropospheric methane between 1841 and 1978 from a high accumulation-rate Antarctic ice core, *Tellus, Ser. B*, 44, 282–294, 1992.
- Fenchel, T., G. M. King, and T. H. Blackburn, *Bacterial Biogeochemistry: The Ecophysiology of Mineral Cycling*, 307 pp., Academic, San Diego, Calif., 1998.
- Frenzel, P., Methyl fluoride, an inhibitor of methane oxidation and methane production, *FEMS Microbiol. Ecol.*, 21, 25–36, 1996.
- Hansen, J. E., M. Sato, A. Lacis, R. Ruedy, I. Tegen, and E. Matthews,

- Climate forcings in the Industrial era, *Proc. Natl. Acad. Sci.*, 95, 12,753–12,758, 1998.
- Hanson, R. S., and T. E. Hanson, Methanotrophic bacteria, *Microbiol. Rev.*, 60(2), 439–471, 1996.
- Harries, J. E., H. E. Brindley, P. J. Sagoo, and R. J. Bantges, Increases in greenhouse forcing inferred from the outgoing longwave radiation spectra of the Earth in 1970 and 1997, *Nature*, 410, 355–357, 2001.
- Hart, S. C., D. Binkley, and D. A. Perry, Influence of red alder on soil nitrogen transformations in two conifer forests of contrasting productivity, *Soil Biol. Biochem.*, 29(7), 1111–1123, 1997.
- Hoefs, J., *Stable Isotope Geochemistry*, 220 pp., Springer-Verlag, New York, 1997.
- Houghton, J. T., L. G. Meira Filho, B. A. Callander, N. Harris, A. Kattenberg, and K. Maskell, *Climate Change 1995: The Science of Climate Change*, Cambridge Univ. Press, New York, 1996.
- King, G. M., In situ analyses of methane oxidation associated with the roots and rhizomes of a bur reed, *Sparganium eurycarpum*, in a Maine wetland, *Appl. Environ. Microbiol.*, 62(12), 4548–4555, 1996.
- King, G. M., Responses of atmospheric methane consumption by soils to global climate change, *Global Change Biol.*, 3, 351–362, 1997.
- Kirkham, D., and W. V. Bartholomew, Equations for following nutrient transformations in soil, utilizing tracer data, *Soil Sci. Soc. Am. Proc.*, 18, 33–34, 1954.
- Kirkham, D., and W. V. Bartholomew, Equations for following nutrient transformations in soil, utilizing tracer data, II, *Soil Sci. Soc. Am. Proc.*, 19, 189–192, 1955.
- Lelieveld, J., P. J. Crutzen, and F. J. Dentener, Changing concentration, lifetime and climate forcing of atmospheric methane, *Tellus, Ser. B*, 50, 128–150, 1998.
- Liptay, K., J. Chanton, P. Czepiel, and B. Mosher, Use of stable isotopes to determine methane oxidation in landfill cover soils, *J. Geophys. Res.*, 103(D7), 8243–8250, 1998.
- Madsen, E. L., Epistemology of environmental microbiology, *Environ. Sci. Technol.*, 32, 429–439, 1998.
- Mathews, E., Wetlands, in *Atmospheric Methane*, edited by M. A. K. Khalil, Springer-Verlag, New York, 2000.
- Mathews, E., and I. Fung, Methane emission from natural wetlands: Global distribution, area, and environmental characteristics, *Global Biogeochem. Cycles*, 1(1), 61–86, 1987.
- Moosavi, S. C., and P. M. Crill, CH₄ oxidation by tundra wetlands as measured by a selective inhibitor technique, *J. Geophys. Res.*, 103(D22), 29,093–29,106, 1998.
- Neill, C., M. C. Piccolo, J. M. Melillo, P. A. Steudler, and C. C. Cerri, Nitrogen dynamics in Amazon forest and pasture soils measured by N-15 pool dilution, *Soil Biol. Biochem.*, 31(4), 567–572, 1999.
- Neter, J., W. Wasserman, and M. H. Kutner, *Applied Linear Statistical Models: Regression, Analysis of Variance and Experimental Designs*, 1181 pp., Irwin, Burr Ridge, Ill., 1990.
- Oremland, R. S., and C. W. Culbertson, Evaluation of methyl fluoride and dimethyl ether as inhibitors of aerobic methane oxidation, *Appl. Environ. Microbiol.*, 58(9), 2983–2992, 1992a.
- Oremland, R. S., and C. W. Culbertson, Importance of methane-oxidizing bacteria in the methane budget as revealed by the use of a specific inhibitor, *Nature*, 356, 421–423, 1992b.
- Perakis, S. S., and L. O. Hedin, Fluxes and fates of nitrogen in soil of an unpolluted old-growth temperate forest, southern Chile, *Ecology*, 82(8), 2245–2260, 2001.
- Peters, V., and R. Conrad, Methanogenic and other strictly anaerobic bacteria in desert soil and other oxic soils, *Appl. Environ. Microbiol.*, 61(4), 1673–1676, 1995.
- Petit, J. R., et al., Climate and atmospheric history of the past 420,000 years from the Vostok ice core, Antarctica, *Nature*, 399, 429–436, 1999.
- Potter, C. S., An ecosystem simulation model for methane production and emission from wetlands, *Global Biogeochem. Cycles*, 11(4), 495–506, 1997.
- Potter, C. S., E. A. Davidson, and L. V. Verchot, Estimation of global biogeochemical controls and seasonality in soil methane consumption, *Chemosphere*, 32(11), 2219–2246, 1996.
- Rimbault, A., P. Niel, H. Virelizier, J. C. Darbord, and G. Leluan, L-Methionine, a precursor of trace methane in some proteolytic Clostridia, *Appl. Environ. Microbiol.*, 54(6), 1581–1586, 1988.
- Roslev, P., N. Iversen, and K. Henriksen, Oxidation and assimilation of atmospheric methane by soil methane oxidizers, *Appl. Environ. Microbiol.*, 63(3), 874–880, 1997.
- Saarnio, S., J. Alm, J. Silvola, A. Lohila, H. Nykanen, and P. J. Martikainen, Seasonal variation in CH₄ emissions and production and oxidation potentials at microsites on an oligotrophic pine fen, *Oecologia*, 110, 414–422, 1997.
- Schuur, E. A. G., O. A. Chadwick, and P. A. Matson, Carbon cycling and soil carbon storage in mesic to wet Hawaiian montane forests, *Ecology*, 82, 3182–3196, 2001.
- Sexstone, A. J., N. P. Revsbech, T. B. Parkin, and J. M. Tiedje, Direct measurement of oxygen profiles and denitrification rates in soil aggregates, *Soil Sci. Soc. Am. J.*, 49, 645–651, 1985.
- Snover, A. K., and P. D. Quay, Hydrogen and carbon kinetic isotope effects during soil uptake of atmospheric methane, *Global Biogeochem. Cycles*, 14(1), 25–39, 2000.
- Stark, J. M., and S. C. Hart, High rates of nitrification and nitrate turnover in undisturbed coniferous forests, *Nature*, 385, 61–64, 1997.
- Sugimoto, A., T. Inoue, N. Kirtibutr, and T. Abe, Methane oxidation by termite mounds estimated by the carbon isotopic composition of methane, *Global Biogeochem. Cycles*, 12(4), 595–605, 1998.
- Sundh, I., M. Nilsson, G. Granberg, and G. H. Svenson, Depth distribution of microbial production and oxidation of methane in northern boreal peatlands, *Microbial Ecol.*, 27, 253–265, 1994.
- Walter, B. P., and M. Heimann, A process-based, climate sensitive model to derive methane emissions from natural wetlands: Application to five wetland sites, sensitivity to model parameters, and climate, *Global Biogeochem. Cycles*, 14(3), 745–765, 2000.
- Wang, W. C., Y. L. Yung, A. A. Lacis, T. Mo, and J. E. Hanson, Greenhouse effects due to man-made perturbations of trace gases, *Science*, 194(4266), 685–690, 1976.
- Whalen, S. C., W. S. Reebergh, and V. A. Barber, Oxidation of methane in boreal forest soils: A comparison of 7 measures, *Biogeochemistry*, 16, 181–211, 1992.
- Whiticar, M. J., Stable isotopes and global budgets, in *Atmospheric Methane: Sources, Sinks, and Role in Global Change*, edited by M. A. K. Khalil, pp. 138–167, Springer-Verlag, New York, 1993.
- Wieder, R. K., and J. B. Yavitt, Peatlands and global climate change: Insights from comparative studies of sites situated along a latitudinal gradient, *Wetlands*, 14(3), 229–238, 1994.
- Yavitt, J. B., D. M. Downey, G. E. Lang, and A. J. Sexstone, Methane consumption in two temperate forest soils, *Biogeochemistry*, 9, 39–52, 1990.
- Yavitt, J. B., T. J. Fahey, and J. A. Simmons, Methane and carbon dioxide dynamics in a northern hardwood ecosystem, *Soil Sci. Soc. Am. J.*, 59, 796–804, 1995.
- Zinder, S. H., Physiological ecology of methanogens, in *Methanogens: Ecology, Physiology, Biochemistry and Genetics*, edited by J. G. Ferry, pp. 128–206, Chapman and Hall, New York, 1993.

L. O. Hedin, Department of Ecology and Evolutionary Biology and Princeton Environmental Institute, Princeton University, Princeton, NJ 08544, USA. (Lhedin@Princeton.edu)

J. C. von Fischer, Department of Geosciences, Guyot Hall, Princeton University, Princeton, NJ 08544, USA. (jcvf@princeton.edu)